DECORATION OF INDENTATION CRACKS IN 3Y-TZP BY HYDROTHERMAL AGEING

F. García Marro, E. Camposilvan, A. Mestra, and M. Anglada

Dep. Ciencia de los Materiales y Ing. Metalúrgica, Universidad Politécnica de Cataluña
Av. Diagonal, 647, 08028 Barcelona, España
E-mail: fernando.garcia.marro@upc.edu

RESUMEN

Las grietas de indentación en cerámicas son frecuentemente utilizadas no sólo para estimar semi-empíricamente la tenacidad a fractura K_{IC}, sino también cómo método para crear grietas agudas superficiales y semielípticas a partir de las cuales analizar la tenacidad de fractura. Para ello es necesario conocer la forma exacta de la grieta inicial, así como en el momento de fractura inestable. A menudo dicha identificación no es obvia debido a un pobre contraste visual de las superficies fracturadas. La circona estabilizada con 3% molar de itria (3Y-TZP) es una cerámica biocompatible con buenas propiedades mecánicas que la hacen interesante para su utilización en prótesis dentales y cabezas femorales. Adicionalmente, la 3Y-TZP es susceptible a un fenómeno de degradación a baja temperatura por el cual un ambiente acuoso produce una transformación de fase en la superficie expuesta. En este trabajo se ha aprovechado la susceptibilidad a degradación hidrotérmica de la 3Y-TZP para revelar grietas de indentación en probetas que son ensayadas a flexión posteriormente. Se muestra como grietas de indentación en 3Y-TZP afectadas por vapor de agua son claramente reveladas en la posterior caracterización fractográfica. Se consideraron diferentes tipos de 3Y-TZP con diferentes grados de susceptibilidad a degradación hidrotérmica. Se observó que una exposición en autoclave de unas pocas horas es suficiente para revelar las grietas en la superficie de fractura sin llegar a afectar la carga de rotura de las probetas. Por consiguiente, la técnica puede utilizarse para obtener un conocimiento preciso de la geometría de las grietas de indentación utilizadas para determinar la tenacidad de fractura.

ABSTRACT

Indentation cracks on ceramics are frequently used not only for the semi-empirical determination of the fracture toughness K_{IC} but also as a method for generating semielliptical surface cracks to be used in as starting cracks in fracture and fatigue studies. Tetragonal zirconia stabilized with 3 % mol of yttria (3Y-TZP) is a biocompatible ceramic with good mechanical properties which is used in dental and femoral prostheses applications. Additionally, 3Y-TZP is susceptible to low temperature degradation in which a hydrothermal environment induces a phase transformation of the exposed surface. In the present work, this degradation susceptibility of 3Y-TZP has been used to reveal indentation crack profiles on specimens which were tested by flexural bending afterwards. Different types of 3Y-TZP were considered which presented different degrees of susceptibility to hydrothermal degradation. It is shown that these cracks are clearly decorated by the water vapour which make them easily revealed on the fracture surfaces. An exposition of few hours in autoclave is sufficient for revealing the indentation cracks on the fracture surface without affecting the fracture load of the specimens. Therefore, the method can be applied to visualize with precision the geometry of indentation cracks which are used to determine the fracture toughness.

PALABRAS CLAVE: Cerámicas, Resistencia, Biomateriales

1. INTRODUCTION

Indentation cracks have been frequently used to study the fracture toughness of ceramics either from the indentation crack length or from the strength of indented pre-cracked specimens (surface crack in flexure (SCF) methods) [1]. In such a strength test, it is essential to make sure that the indentation residual stresses are previously removed either by removing the plastic zone or annealing the indented specimen. In SCF test methods it is also necessary to determine the starting crack geometry for a posterior fracture mechanics analysis. However, the initial position of the crack is frequently difficult to visualize during the post-mortem fractographic examination due to poor visual contrast.

Environmentally assisted slow crack growth may also be present after the indentation or when the stress is raised in strength testing at room-temperature, and this opens the question of the actual crack dimensions that have to be considered in the analysis. Swab and Quinn [2] studied in 1998 the fracture surfaces of different indented ceramics after strength testing at room temperature showing the presence of what they called "halos" around the periphery of indentation cracks. In some of the ceramics studied (alumina and glass) this halo was attributed to environmentally-assisted slow crack growth while in others it was attributed to slow crack growth under the indentation-induced residual stresses.

In polycrystalline tetragonal zirconia stabilized with 3 % molar yttria (3Y-TZP) it is not easy to identify the initial crack on the fracture surface of an indented pre-cracked specimen. Halos around indentation cracks are not usually observed for this ceramic in spite of presenting substantial slow crack growth behaviour at room temperature [3]. Susceptibility to hydrothermal ageing is a distinctive feature of 3Y-TZP [4]-[8], which consists in the formation of monoclinic phase on the surface during exposure to humid environments. This phenomenon is referred to as "low temperature degradation" (LTD) or as "hydrothermal ageing" of TZP ceramics. The surface subjected to LTD becomes highly microcracked, the kinetics of ageing in air is maximal around 250 °C and there is evidence that ageing is also operative at much lower temperatures [5], [9]. The micro-cracked zone growths with ageing time producing a decrease on the tribological properties after short times of ageing and a reduction on the flexural strength after long times. If the ageing conditions are aggressive enough, the specimen can even disintegrate. For example, Boukis *et al* [10] investigated the corrosion resistance of Y-TZP in simulated supercritical water oxidation environment at 465 °C at the pressure of 25 MPa. Under these severe conditions, the ceramic just disintegrated. Under less severe conditions, Kojima *et al* [11] found that 3Y-TZP sintered at more than 1550 ºC disintegrated under ageing in a range between 200 °C and 400 °C and at a pressure of 30 MPa. The degree of disintegration depended on the grain size of the 3Y-TZP and the ageing temperature.

If an indentation crack in 3Y-TZP is exposed to water vapour, it is expected that the exposed crack surfaces will transform to monoclinic phase in a similar way as the specimen surface. Recently, we have observed [12] a strong contrast on the fracture surface in the periphery of the indentation crack in commercial 3Y-TZP subjected to ageing. In that work, we focused on the changes in the fracture strength in indented specimens after long ageing times.

In the present work, we focus on the visual contrast produced by water vapour exposure in the periphery of indentation cracks. This was studied in different 3Y-TZP ceramics with different susceptibilities to hydrothermal degradation. One of these ceramics was actually completely resistant to degradation and it will be shown how, even in this case, the water exposure was effective in staining the crack. Therefore, this crack decoration technique might be used to mark crack profiles in indented ceramic specimens tested for the determination of fracture toughness, as far as it can be proved that the hydrothermal exposure for short times has a negligible influence on the strength.

2. EXPERIMENTAL

Commercial TZ-3YSB-E powder (Tosoh Co., Japan) was cold isostatic pressed at 200 MPa producing green compact bars which were sintered in an alumina tube furnace (Hobersal ST-18) with heating and cooling rates of 3 ºC/min. Two sintering temperatures were used: 1450 ºC and 1550 ºC, producing in this way two final bars with different grain size (named here as AS5 and AS7 respectively). A third material (AS3) was produced from the same starting powder by presintering at 1200 ºC producing a body with ~35 % apparent porosity as measured by mercury intrusion porosimetry. The porous bar was cut into discs of 2 mm thickness using only distilled water as lubricant, the discs were then immersed in a solution of 50 % wt. cerium salt solution in ethanol (Alfa Aesar Cerium III Nitrate Hexahydrate). After immersion of the discs for 10 minutes, they were dried at 200 ºC for 1 hour and then finally sintered at 1450 ºC for 2 hours. The final specimens produced in this way contained 2.5 % wt cerium on their surface as analysed by Electron Probe Micro Analysis (EPMA Cameca sx50). This AS3 condition possessed a similar grain size as AS5 but lower t-m phase transformability at the surface. CeO_2 is a stabilizer of the tetragonal phase, inducing lower fracture toughness and decreasing the susceptibility to ageing due to its higher phase stability. The reason to choose AS3 was to study the effect of hydrothermal exposure on the indentation crack when no ageing occurs. AS3, AS5 and AS7 possessed different fracture toughness; the numbers 3, 5 and 7 next to "AS" indicate the value of the indentation fracture toughness of each material. All these conditions presented different susceptibilities to hydrothermal ageing.

Indentation fracture toughness in air, K_{IC}, was determined by Vickers indentation at different loads of 5, 10, 20 and 40 kg; which produced cracks at the imprint corners. For AS5 and AS7, the cracks were of Palmqvist type and K_{IC} was determined with the expression proposed by Niihara *et al* [13]:

$$K_{IC} = 0.025(E/H)^{0.4}\left(\frac{PH}{8c}\right)^{1/2}; \quad 1 \le \frac{2c}{d} \le 2.5 \quad (1)$$

where d is the imprint semi-diagonal, $2c$ the observed crack length at the surface (distance from imprint corner to crack tip), E is the Young modulus and the hardness parameter stands for $H=P/2d^2$ (P is the indentation load). For AS5 it was obtained K_{IC} = 5.1 ± 0.1 MPa√m, while the coarse-grained material AS7 showed a higher fracture toughness K_{IC} = 6.9 ± 0.2 MPa√m. For AS3, the indentation cracks were connected below the imprint and K_{IC} in this case was determined with the expression proposed by Anstis [14]:

$$K_{IC} = 0.016(E/H)^{1/2}Pc^{-3/2} \quad (2)$$

Here c represents the radius of the half-penny crack. For AS3, it was then obtained K_{IC} = 2.9 ± 0.1 MPa√m (3.8 ± 0.1 MPa√m, in case Niihara expression is used). Although indentation methods give only rough estimations of the actual fracture toughness [15], it is clear that fracture toughness increases in the order AS3, AS5 and AS7.

From the sintered cylindrical bars, discs were obtained with 10 mm diameter and 2 mm thickness, which were polished up to colloidal silica achieving a mirror-like finishing. The Young modulus was 230 GPa for all materials as measured by the impulse excitation technique (GrindoSonic MK5i) and the bulk density was over 99 % of the theoretical value as determined by the Archimedes method. Other properties are given in table 1. All materials had a fully tetragonal microstructure; however, the existence of a small amount of cubic phase cannot be ruled out because of the overlapping of the cubic and tetragonal phases.

Table1: average grain size, 1 kg Vickers hardness and monoclinic content at the surface after exposure in autoclave at 131 ºC for 100 hours.

Material	Grain size (μm)	HV1 (GPa)	V_m
AS3	0.30	12,0	0 %
AS5	0.30	12,0	80 %
AS7	0.85	16,0	80 %

The specimens were indented at the centre with a 10 kg load, producing Palmqvist cracks at the imprint corners in AS5 and AS7, but in AS3 they were half-penny cracks as previously mentioned. Fracture on the specimens was controlled by these cracks, since they were much larger than the critical defect size. In order to remove the indentation residual stresses, only AS5 specimens were annealed at 1200 °C for 1 hour after indentation. Afterwards, the specimens were hydrothermally aged by exposure to 100 % steam atmosphere in autoclave at 131 ºC and 2 bar pressure for different times up to 100 hours. AS3 and AS7 indented specimens were also hydrothermally aged under the same conditions, but without a previous annealing. In order to determine the monoclinic content at the surface of the specimens, X-ray diffraction (XRD) was performed on the aged discs with Cu K_α incident radiation (1.5406 Å) in symmetric θ-2θ configuration with a Bruker AXS D8 diffractometer. From the XRD spectra, the monoclinic volume fraction was then determined as [16]:

$$Vm = \frac{1.311(I_m^{111} + I_m^{\bar{1}11})}{I_t^{111} + 1.311(I_m^{111} + I_m^{\bar{1}11})} \qquad (3)$$

Here, I_t and I_m represent the intensities of the (111) tetragonal and of either (-111) or (111) monoclinic peaks, respectively. To study the effect of water vapour exposure on the strength of the indented discs, these were broken by a ball-on-three ball test in an Instron 8511 machine with WC balls of 6 mm diameter at 20 N/s loading rate. For this biaxial flexural test, the stresses in the disc centre have been previously determined by finite element analysis by Börger *et al* [17], [18]. The maximum stress at the disc centre can be obtained from the following expression [19]:

$$\sigma_{\max} = \frac{3F}{4\pi t^2}\left[2(1+\nu)\ln(R/\alpha t) + (1-\nu)\ln((R/R_D)^2)\right] \quad (4)$$

where F is the applied load, $\nu = 0.33$ is the Poisson's ratio, R_D and t represent the disc radius and thickness respectively, and R is the support radius (distance from the disc centre to the support points). The parameter α ensures an equi-biaxial stress state in the specimen centre; a value of $\alpha = 0.2$ was suggested by Fett *et al* [19] from FE-results reported by Shetty *et al* [20] for $R/R_D = 0.75$, $\nu = 0.3$, and $t/R_D = 0.1$. The fracture surfaces of the broken disc specimens were observed by laser scanning confocal microscopy (LSCM, Olympus Lext) and then by scanning electron microscopy (SEM, JEOL JSM 6400).

Figure 1 shows top views of two indented AS5 specimens; the left image is an indented disc showing the indentation cracks, the other image shows a portion of an indented disc just after fracture by the biaxial flexural test. All indented discs fractured into two half-pieces, and in this figure it can be appreciated how the fracture plane corresponds to one indentation crack plane, thus enabling their posterior visualization as appreciated in the following images.

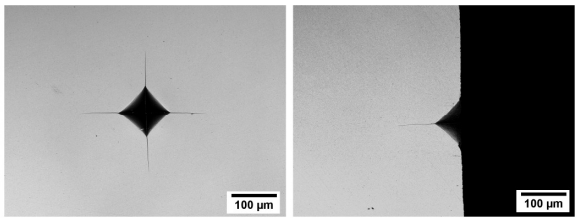

Figure 1: Fracture of an indented specimen.

3. RESULTS

As a consequence of the different microstructure or/and composition; the three TZP ceramics studied here showed different susceptibility to LTD degradation. The susceptibility to degradation was evaluated considering the growth rate of the degraded layer with hydrothermal exposure, as observed from the fracture surfaces of broken specimens. This visual layer is known to be rich in monoclinic content due to the water-induced phase transformation; however, it does not exactly correspond to the monoclinic content profile [21]; it rather indicates the depth of the specimen up to which the structural integrity has been affected by the water species so that the fracture mode becomes completely intergranular.

Figure 2 shows the growth of the surface degraded layer with ageing time for the different material conditions. Low toughness AS3 was resistant to ageing even after 100 h of hydrothermal exposure, as revealed by the lack of degraded layer on the fracture surfaces. Characterization by XRD showed no monoclinic phase content on the AS3 specimens after the longest hydrothermal exposure (see Table 1). On the other hand, AS5 (which corresponds to the standard grade 3Y-TZP)

was susceptible to ageing, showing a degraded layer of about 9 µm after 100 h of hydrothermal exposure. After this time, the monoclinic content was up to 80 % on the surface of the specimens. The AS7 ceramic was the most susceptible to ageing, presenting a degraded layer of about 20 µm after 100 h of hydrothermal exposure. As explained before, AS7, which has the coarser grain size, was also the most degraded, due to the well established relationship between transformability and grain size [4], [22]-[24].

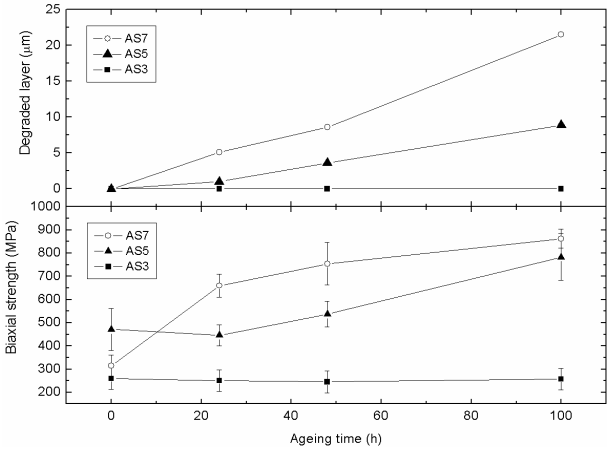

Figure 2: Change with ageing time of the thickness of the surface degraded layer (upper graph) and biaxial strength of indented specimens in terms of ageing time (lower graph).

Figure 2 also shows the evolution of the biaxial strength of indented specimens with the exposure time in autoclave. For AS3, the initial strength of indented specimens before autoclaving was around 260 ± 50 MPa, and it remained the same even after the longest exposure to autoclave. The strength of AS3 was the lowest one, as compared to AS5 and AS7, because it has lower fracture toughness and the indentation crack is half-penny (as shown below in figures 3, 4 and 5). On the other hand, the indented and annealed AS5 specimens had an initial strength (without autoclaving) of 470 ± 90 MPa. It should be outlined here again that these specimens were annealed at 1200 ºC in order to remove any indentation residual stress. No change in the strength was found in AS5 after only a few hours of autoclaving, however, after 48 h the strength began to increase substantially. Indeed, after 100 h it had increased up to 700 MPa. This increase in strength of indented specimens with ageing cannot be explained by relaxation of the indentation residual stresses by ageing, as these were initially removed by annealing as mentioned previously. The reason for this strength increase in AS5 has been addressed elsewhere [12]. It can be seen that the effect is even stronger in AS7 whose strength is more than 700 MPa only after a few hours of autoclaving. However, for ageing periods longer than 50 hours, the strength of AS7 practically did not increase any further as can be appreciated in figure 2.

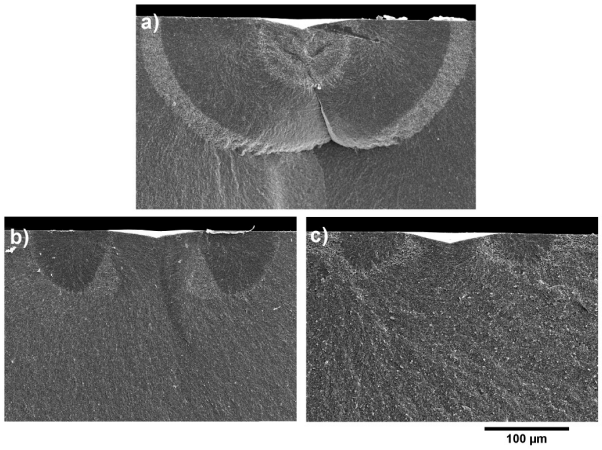

Figure 3: SEM micrographs showing the fracture surface of indented (10 kg) specimens exposed for 100 hours to LTD: a) AS3, b) AS5, c) AS7.

The fracture surfaces of the indented discs subjected to LTD were visualized by SEM (figure 3). This allowed confirmation of previous findings in non-annealed AS5 [12], where it was observed that the edge of the indentation cracks becomes marked if the indented specimen had been hydrothermally exposed. For AS3 a bright and wide "halo" could be clearly observed around the periphery of the indentation crack (figure 3a). Close inspection revealed that this halo corresponds to a zone of intergranular fracture. However, no degraded layer appears on the specimen surface or on the fracture surface. This absence of degraded layer is coherent with the fact that the AS3 condition is resistant to ageing. In this low-toughness material, the revealed cracks are half-penny type (connected below the imprint), and the crack depth is about 145 µm.

The fracture surface of the indented, annealed and aged AS5 specimens also presents a bright contrast around the edge of the indentation crack as observed by SEM (figure 3b). It can also be appreciated that AS5 is susceptible to hydrothermal degradation by the presence of the degraded layer with intergranular fracture close to the surface of the discs (outside the indentation region). Close inspection of the contrasted region in front of the indentation crack edge revealed again that the fracture is intergranular. In this higher toughness material condition, the cracks induced by the indentation can be appreciated to be of Palmqvist type (not connected below the imprint) with a depth of 73 µm. Finally, the fracture surface of the AS7 specimens (figure 3c) clearly manifests their higher toughness by the smaller size of the indentation cracks, which are also of Palmqvist type and with a depth of only 44 µm. This material was the most susceptible to degradation showing the largest degraded layer at the surface.

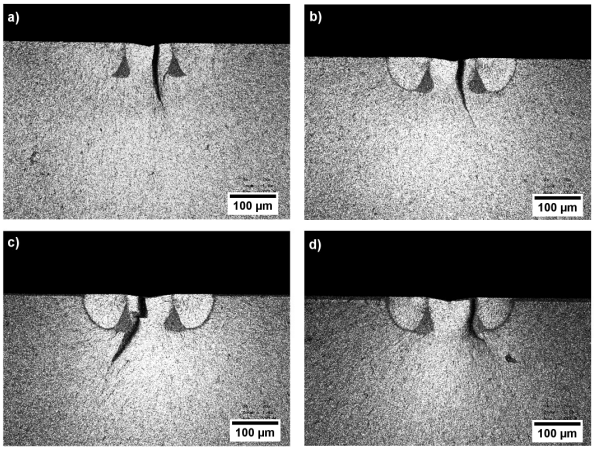

Figure 4: LSCF micrographs showing the fracture surfaces of indented(10 kg) AS5 specimens exposed to water vapour in autoclave for different periods of time: a) no ageing b) 24 h c) 48 h d) 100h.

Figure 4 shows the fracture surfaces of indented AS5 specimens subjected to different ageing times, as observed by LSCM microscopy. This figure demonstrates that optical microscopy is sufficient in order to appreciate the contrast around the edge of the crack. If the indented specimens are not autoclaved, then their fracture surfaces show practically no contrast, being difficult to appreciate the crack (figure 4 a). After 24 h of exposure in autoclave, a thin dark zone can be appreciated around the crack similar to that present near the specimen surface. It corresponds to the bright contrast that can be appreciated by SEM. The different appearance by using the two different microscopy techniques is because they produce different contrast on the same area: in SEM, an intergranular fracture zone of a non-conducting specimen appears in brighter contrast due to electrical charging of the surface at that location, while in optical microscopy the same zone appears as dark since a higher roughness surface is less reflective to light. For longer exposures in autoclave (48 h and 100 h), the dark zone around the crack edge and the degraded layer on the specimen surface both increase. These images show that only 24 h of exposure to water vapour in autoclave is sufficient to clearly reveal indentation cracks on the fracture surface of standard 3Y-TZP, as examined simply by optical microscopy.

It is worth emphasizing that AS3 specimens were resistant to ageing so that water vapour did not induce any t-m transformation on the edge of indentation cracks. However, the dimensions of the indentation crack increased during autoclaving. It was actually observed that the 10 kg indentation crack increased its length from 110 µm to about 150 µm after hydrothermal exposure. Close to the initial position of the crack there was a marked intergranular fracture path, suggesting subcritical crack growth induced by the hydrothermal exposure. Therefore, environmentally assisted slow crack growth occurs in AS3 during hydrothermal exposure without any detectable t-m transformation.

4. CONCLUSIONS

Exposure to hot water vapour is useful for revealing the profiles of indentation cracks in tetragonal polycrystalline zirconia. The procedure was illustrated in 3Y-TZP specimens of different grain size with Palmqvist indentation cracks of different shape. The crack profile is clearly revealed on the fracture surfaces after flexural testing if the specimens are previously exposed to 131 ºC water vapour in autoclave. The contrast is produced by intergranular fracture in a region in front of the initial position of the crack tip. In transformable 3Y-TZP this effect is induced by tetragonal-to-monoclinic phase transformation during the water vapour exposure. After long ageing times, the biaxial strength and corresponding apparent fracture toughness increase substantially. On the other hand, in TZP resistant to low temperature degradation (produced by ceria addition to Y-TZP) the position of the crack can be detected by the change in fracture path that takes place by subcritical crack growth during exposure to water vapour.

ACKNOWLEDGEMENTS

The authors acknowledge the financial support from the Ministerio de Ciencia e Innovación (MICINN) of Spain through project MAT2008-03398 and the partial grant given to F. G. Marro. E. Camposilvan acknowledges Universitat Politècnica de Catalunya for the grant UPC_FPU. The general financial support to the research group given by the Generalitat de Catalunya is also acknowledged (2009SGR01285).

REFERENCES

[1] Quinn G. D., Gettings R. J., Kübler J. J., *Fracture toughness of ceramics by the surface crack in flexure (SCF) method*, Fracture Mechanics of Ceramics, 11, pp. 203-218, 1996.

[2] Swab J., Quinn G. D., *Effect of crack ''halos'' on fracture toughness determined by the surface crack in flexure method,* J. Am. Ceram. Soc., 81, pp. 2261-2268, 1998.

[3] Chevalier J., Olagnon C., Fantozzi G., *Subcritical crack propagation in 3Y-TZP ceramics: static and cyclic fatigue*, J. Am. Ceram. Soc., 82, pp. 3129-3138, 1999.

[4] Chevalier J., Gremillard L., Deville S., *Low-temperature degradation of zirconia and implications for biomedical implants*, Annual Review of Materials Research, 37, pp. 1-32, 2007.

[5] Kobayashi K., Kuwajima H., Masaki T., *Phase change and mechanical properties of ZrO_2-Y_2O_3 solid electrolyte after ageing*, Solid State Ion 3/4, pp. 489–493, 1980.

[6] Marro F. G., Valle J., Mestra A., Anglada M., *Surface modification of 3Y-TZP with cerium oxide,* J. Eur. Ceram. Soc. 31, pp. 331-338, 2011.

[7] Marro F. G., Mestra A., Anglada M., *Contact damage in a Ce-TZP/Al_2O_3 nanocomposite,* J. Eur. Ceram. Soc., 31, pp. 2189-2197, 2011.

[8] Marro F. G., Chintapalli R., *Study of near surface changes in YTZP after LTD*, Int. J. Mat. Res., 100, pp. 92-96, 2009.
[9] Sergo L. V., *Low temperature degradation ageing of zirconia: A critical review of the relevant aspects in dentistry*, Dental Materials, 26, pp. 922-928, 2010.
[10] Boukis N., Claussen N., Ebert K., Janssen R., Schacht M., *Corrosion screening tests of high-performance ceramics in supercritical water containing oxygen and hydrochloric acid*, J. Eur. Ceram. Soc., 17, pp. 71, 1997.
[11] Kojima T., Mori Y., Kamiya M., Sasai R., Itoh H., *Disintegration process of yttria-stabilized zirconia ceramics using hydrothermal conditions*, J. Mater. Sci., 42, pp. 6056-6061, 2007.
[12] Marro F. G., Anglada M., *Strengthening of Vickers indented 3Y-TZP by hydrothermal ageing,* J. Eur. Ceram. Soc., 32, pp. 317-324, 2012.
[13] Niihara K., Morena R., Hasselman D. P. H., *Evaluation of K_{IC} of brittle solids by the indentation method with low crack-to-indent ratios*, J. Mater. Sci. Letters, 1, pp. 13-16, 1982.
[14] Anstis G. R., Chantikul P., Lawn B. R., Marshall D. B., *A critical evaluation of indentation techniques for measuring fracture toughness: I, Direct crack measurements*, J. Am. Ceram. Soc., 64, pp. 533-538, 1981.
[15] Quinn G. D., Bradt R. C., *On the Vickers indentation fracture toughness test*, J. Am. Ceram. Soc., 90, pp. 673-680, 2007.
[16] Toraya H., Yoshimura M., Somiya S., *Calibration curve for quantitative analysis of the monoclinic-tetragonal ZrO_2 system by X-ray diffraction*, J. Am. Ceram. Soc., 67, pp. C119-C121, 1984.
[17] Börger A., Supancic P., Danzer R., *The ball on three balls test for strength testing of brittle discs: stress distribution in the disc,* J. Eur. Ceram. Soc. 22, pp. 1425-1436, 2002.
[18] Börger A., Supancic P., Danzer R., *The ball on three balls test for strength testing of brittle discs: part II: analysis of possible errors in the strength determination*, J. Eur. Ceram. Soc., 24, pp. 2917-2928, 2004.
[19] Fett T., Rizzi G., Esfehanian M., Oberacker R., *Simple expressions for the evaluation of stresses in sphere-loaded discs under biaxial flexure,* J. Test. Eval., 36, pp. 285-290, 2008.
[20] Shetty K. D., Rosenfield A. R., McGuire P., Duckworth W.H., *Biaxial flexure test for ceramics*, Am. Ceram. Soc. Bull., 59, pp. 1193-1197, 1980.
[21] Muñoz-Tabares A., Jimenez-Pique E., Anglada M., *Subsurface evaluation of hydrothermal degradation of zirconia*, Acta Materialia*,* 59, pp. 473-484, 2011.
[22] Watanabe M., Iio S., Fukuura I., *Ageing behaviour of Y-TZP*, In Advances in Ceramics, Vol. 12, Science and Technology of Zirconia II, ed. N. Claussen, M. Ruhle & A. H. Heuer, The American Ceramic Society, Inc., Columbus, Ohio, pp. 391-398, 1984.
[23] Lawson S., *Environmental degradation of zirconia ceramics*, J. Eur. Ceram. Soc., 15, pp. 485-502, 1995.
[24] Gaillard Y., Jimenez-Pique E., *Quantification of hydrothermal degradation in zirconia by nanoindentation,* Acta Materialia, 56, pp. 4206-4216, 2008.